ELSEVIER

Materials Science and Engineering A231 (1997) 48–54

MATERIALS SCIENCE & ENGINEERING A

# Structure of mullite coatings grown by chemical vapor deposition

D. Doppalapudi, S.N. Basu *

*Manufacturing Engineering Department, Boston University, 15 St. Mary's Street, Boston MA 02215, USA*

Received 9 August 1996; revised 10 February 1997

**Abstract**

Dense mullite coatings have been deposited on SiC and $Si_3N_4$ substrates by chemical vapor deposition (CVD). The coatings were compositionally graded with the Al/Si ratio increasing from 1.5 at the substrate/coating interface, to a value of 8 at the coating surface. This gradation of composition is discussed in light of changes in the concentration of oxygen vacancies, ordering of the vacancies, formation and size of domains and the observed changes in lattice parameters. © 1997 Elsevier Science S.A.

*Keywords:* Chemical vapor deposition; Mullite coating; Structure

## 1. Introduction

Silicon-based ceramics (SiC and $Si_3N_4$) are widely used for high temperature applications such as heat exchangers, gas turbines and internal combustion engines, due to their high strength and thermal conductivity, as well as thermal shock and oxidation resistance at temperatures above 1000°C. However, they need protective coatings due to their failure by hot corrosion and contact stress damage. Mullite ($3Al_2O_3 \times 2SiO_2$) is an excellent candidate material for such coatings, by virtue of its coefficient of thermal expansion (CTE) match with the substrates, in particular with SiC (mullite has CTE value of $5.05 \times 10^{-6}°C^{-1}$, compared to $4.7 \times 10^{-6}°C^{-1}$ for SiC and $3.0 \times 10^{-6}°C^{-1}$ for $Si_3N_4$ [1]). Mullite also has high creep and thermal shock resistance, excellent chemical stability, strength as well as oxidation and corrosion resistance at elevated temperatures [2].

Mullite is the only thermodynamically stable phase at atmospheric pressure in the $SiO_2$—$Al_2O_3$ system [3]. It has a high melting point (around 1850°C) and retains its strength up to 1500°C. Mullite is a non-stoichiometric compound with a range of equilibrium solid solubility. In-spite of extensive research, there is still substantial disagreement over the range of solid solubility of mullite. As reported by Aramaki and Roy, mullite generally exists between the limits of $3Al_2O_3 \times 2SiO_2$ and $2Al_2O_3 \times SiO_2$ [4]. The non-stoichiometry of mullite is adjusted by changes in oxygen vacancy concentration [5]. In general, mullite has the chemical formula:

$$Al_2^{VI}(Al_{2+2x}^{IV}Si_{2-2x}^{IV})O_{10-x} \quad (1)$$

where $x$ denotes the number of oxygen vacancies per unit cell and IV and VI are the coordination states of the cations. The parameter $x$ is related to Al/Si ratio as:

$$x = \frac{(\frac{Al}{Si} - 2)}{(\frac{Al}{Si} + 1)} \quad (2)$$

At the above mentioned solubility limits, the values of Al/Si are 3 ($x = 0.25$) and 4 ($x = 0.4$), respectively. The Al/Si ratio is a useful parameter to describe mullite composition during X-ray and electron microscopy investigations, since Al and Si have very similar atomic weights and their peaks in energy dispersive spectra are effected similarly by factors such as specimen thickness.

Several researchers have claimed that mullite may be found over a wider composition range than mentioned above. For example, Aksay and Pask [6] reported a Al/Si ratio of 2.8, which is the lowest reported. Prochazka and Klug [7] reported a shift in solubility range towards higher $Al_2O_3$ content, with increasing temperature. Li et al. [8] reported metastable mullite with Al/Si ratio of 6, which precipitated out $Al_2O_3$ upon annealing. Cameron [5] analyzed mullite with an Al/Si ratio as high as 6.4. He also found that when he

* Corresponding author. Tel.: +1 617 3536728; fax: +1 617 3535548.


*PII* S0921-5093(97)00075-0

extrapolated his experimental data on alumina rich mullite to pure $Al_2O_3$, the unitcell dimensions matched with those of $\eta$-alumina. His findings were in agreement with Burnham's [9] assertion that mullite solid solution, in theory, could extend fully between sillimanite ($Al_2O_3 \times SiO_2$) and pure alumina.

Mullite has an orthorhombic structure with lattice parameters of $a = 0.7546$, $b = 0.7690$ and $c = 0.288$ nm [10]. The symmetry of this structure belongs to space group pbam (no. 55). The crystal structure of mullite is a modified defect structure of sillimanite ($Al_2O_3 \times SiO_2$) in which the particular mullite stoichiometry is achieved by substituting some of the $Si^{4+}$ ions with $Al^{3+}$ [5,11–16]. The resulting charge imbalance is incorporated by introduction of oxygen vacancies.

Ordering of oxygen vacancies can occur under certain processing conditions. Although Schryvers et al. [15] asserted that vacancies are randomly distributed in mullite, Cameron and Morimoto et al. [5,17] have claimed that the solid solutions with high aluminium compositions are stabilized by the ordering of oxygen vacancies. The ordering phenomenon leads to extra reflections around {h01} spots in diffraction patterns [5,13,16]. In mullites with high alumina content (Al/Si = 5 to 6), the existence of anti-phase boundaries (APB) and domains have been observed [17]. Twinning was also reported by some authors, in high alumina mullites [18].

Pask [3] concluded that formation of homogeneous mullite coatings requires deposition of alumina and silica mixed at the molecular level, followed by a heat treatment for crystallization of mullite. Chemical vapor deposition (CVD) is an ideal processing technique to achieve such an outcome and was therefore chosen for this study. In addition, the CVD process leads to denser and more uniform coatings on substrates with complex shapes. To date, adherent mullite coatings have been successfully deposited on silicon-based substrates only by plasma spraying [19].

## 2. Experimental

A CVD process has been developed, based on equilibrium thermodynamic analysis of $AlCl_3$–$SiCl_4$–$CO_2$–$H_2$ system [20], for the deposition of mullite coatings. Deposition of mullite by CVD was carried out at 950°C under a total pressure of 75 torr and the $AlCl_3/SiCl_4$ ratio was varied between 2 and 3. The details of this deposition process are presented elsewhere [21]. Deposition times for the coatings varied from 2 to 3 h. The overall mullite formation reaction is given as:

$$6AlCl_3 + 2SiCl_4 + 13CO_2 + 13H_2 \rightarrow 3Al_2O_3 \times 2SiO_2 + 13CO + 26HCl \quad (3)$$

The composition, morphology, grain structure and the uniformity of the coatings were studied by XRD and SEM. The microstructure and composition of the coatings were analyzed by TEM and STEM, respectively.

In order to prepare electron transparent cross sectional samples of the microscopic studies, coated surfaces were 'sandwiched' by M-bond epoxy, followed by polishing, dimpling and ion milling to perforation in a Gatan Duomill, using 5 kV argon ions. The samples were studied in a JEOL 200CX TEM operated at 200 kV. Chemical analyses of the coatings were carried out in a VG HB603 STEM.

## 3. Results and discussion

The CVD processing technique resulted in coatings that were adherent, uniform, dense and free of gross defects such as cracks and pores. Fig. 1 shows the surface of a typical coating. Preliminary tests indicated that the coatings had excellent adhesion and hot-corrosion resistance ([22]; personal communication with Dr Woo Lee, Oak Ridge National Laboratory).

Fig. 2 is a typical XRD plot of a coating, which shows that the non-substrate peaks match closely with mullite, although the match with sillimanite is also quite good (the similarity between the unit cells of mullite and sillimanite allows the d-spacings to be similar). However, analysis of the electron diffraction patterns confirmed that the coatings were indeed mullite. Fig. 3(b) shows [010] diffraction pattern taken from a grain in the coating. although superlattice spots appear around {101/2} positions, the {101/2} position itself has no spots. Since the unit cell of sillimanite has a $c$-axis lattice parameter that is twice as large as in mullite ($a = 0.7486$, $b = 0.7675$ and $c = 0.5773$ nm [17]), the (101/2) diffraction spot would be present if the coating is sillimanite.

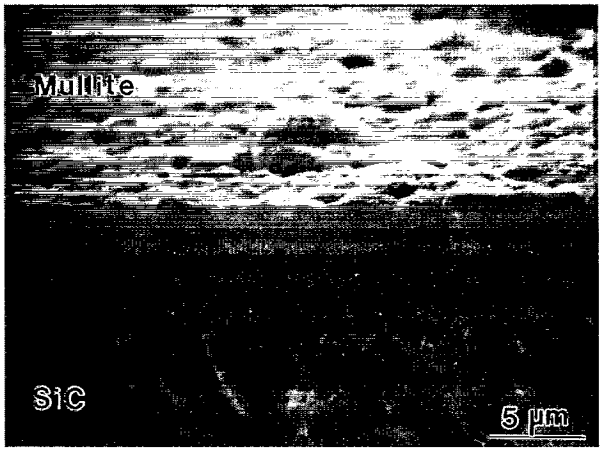


Fig. 1. SEM micrograph of a typical coating of crystalline mullite on a $Si_3N_4$ substrate.

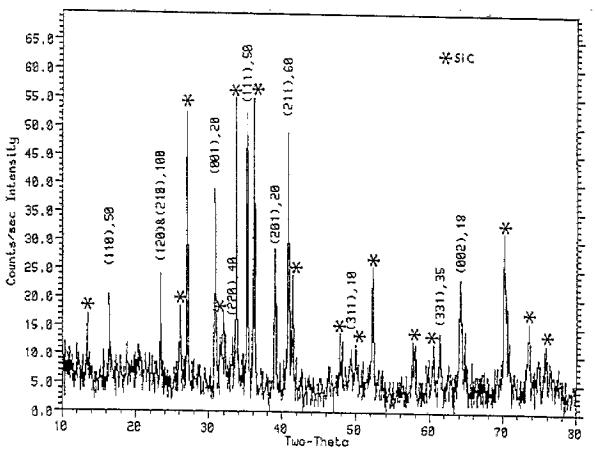


Fig. 2. XRD plot of a mullite coating indicating a [001] texture. The numbers shown are the expected relative intensity values of the corresponding {hkl} planes in randomly oriented polycrystalline mullite.

The measured intensities of the XRD peaks of mullite indicated preferential orientation of the mullite grains. As seen in the Fig. 2, (hk0) planes had a lower intensity, indicating that the (001) planes were preferentially oriented parallel to the interface. In general, grains grow fastest along the shortest lattic parameter ($c$-axis in this case). Thus, it is not surprising that the mullite grains orient themselves such that their $c$-axis is coincident with the growth direction, leading to columnar grain morphology seen in Fig. 3(a).

Fig. 3(a) is a cross-sectional TEM micrograph of a typical mullite coating on SiC. The figure shows the presence of a thin layer near the interface, which does not appear crystalline. However, the electron diffraction from this region, shown in Fig. 3(c), matched well with that of nano-crystalline $\gamma$-$Al_2O_3$. Chemical analysis by STEM using a 40 nm electron probe showed the Al/Si ratio to be around 1.5 at the coating/substrate interface with a steady increase to 2.5 at the top of this nanocrystalline layer. This indicates that the layer is a mixture of two phases, $\gamma$-$Al_2O_3$ and vitreous silica, mixed at a nano-scale. Above the nano-crystalline region, a crystalline layer of columnar mullite grains, 7–10 μm in thickness, was seen in all the coatings. At the nano-crystalline/crystalline grain interface, there was a sharp jump in the Al/Si ratio to 4 followed by a steady increase in this ratio to a value of 8 at the top of the coating.

During the evolution of the coating microstructure, it appears that initially, the deposition of separate phases of $\gamma$-$Al_2O_3$ and vitreous $SiO_2$ occurs, since the Al/Si ratio is insufficient to nucleate mullite. As the Al concentration increases within the nano-crystalline layer, a critical Al/Si ratio is reached, leading to the nucleation of mullite crystals. The thickness of the nanocrystaline layer varied, depending on the coating deposition parameters. This is consistent with the literature, where nucleation of mullite by mixing alumina and silica powders was found to occur when a critical concentration of alumina diffused into silica [23]. It is interesting to note that Chate et al. reported that the formation of mullite is most favored when $\gamma$-$Al_2O_3$ and vitreous $SiO_2$ are used as precursors [24]. Once nucleated, the mullite grains grow with an increasing alumina content with a columnar structure, such that the $c$-axis of the grains is oriented along the deposition direction. The reason behind the steady increase in alumina content in the CVD process is currently under investigation.

To our knowledge, this is the first time that such uniform gradation of the Al/Si ratio within a mullite coating has been reported. Additionally, the Al/Si ratio of 8 within a mullite structure is the highest reported to date. Mullite coatings with such graded composition are expected to have excellent hot-corrosion resistance due to its alumina rich surface. These coatings are expected to have good adherence due to the compatibility of the silica rich inner layer with the native $SiO_2$ layer that exists on all Si-based ceramics. In addition, the CTE gradation, would allow the coatings to have a superior thermal shock resistance as compared to mullite/aluminal dual layer coatings. It is therefore, not surprising that this 'functionally-graded' coating exhibited excellent resistance to hot-corrosion (personal communication with Dr Woo Lee, Oak Ridge National Laboratory).

To understand how mullite can accommodate such large changes in Al/Si ratio without altering the basic structure, the derivation of the stoichiometric mullite ($3Al_2O_3 \times 2SiO_2$) structure needs to be addressed first. The mullite unit cell is a modified defect structure of sillimanite ($Al_2O_3 \times SiO_2$) unit cell. Since the aluminum content in mullite is higher than in sillimanite, mullite can be formed from sillimanite by substituting some of the $Si^{4+}$ ions with $Al^{3+}$ ions and correcting the resulting charge imbalance by the introduction of oxygen vacancy (□) by the reaction:

$$2Si^{4+} + O^{2} \Leftrightarrow 2Al^{3+} + \square \quad (4)$$

Fig. 4 shows the presence of octahedrally coordinated Al atoms ($AlO_6$ octahedra) at the corners and at the center of the unit cell on (00$z$) plane and tetrahedrally coordinated Al and Si atoms in positions marked as $T_1$. The mullite structure is obtained from sillimanite by substituting some of the Si atoms in the tetrahedral ($T_1$) sites by Al. The substitution of Si by Al results in disordering of tetrahedral sites, thereby reducing the value of lattice parameter $c$ to half the value of sillimanite. The oxygen vacancies are introduced only in the $O_c$ type positions, which are shared by two tetrahedra, as can be seen in Fig. 4. Introduction of an oxygen vacancy at this site causes the Al and Si atoms in the $T_1$ sites adjacent to this vacancy to move to a new posi-

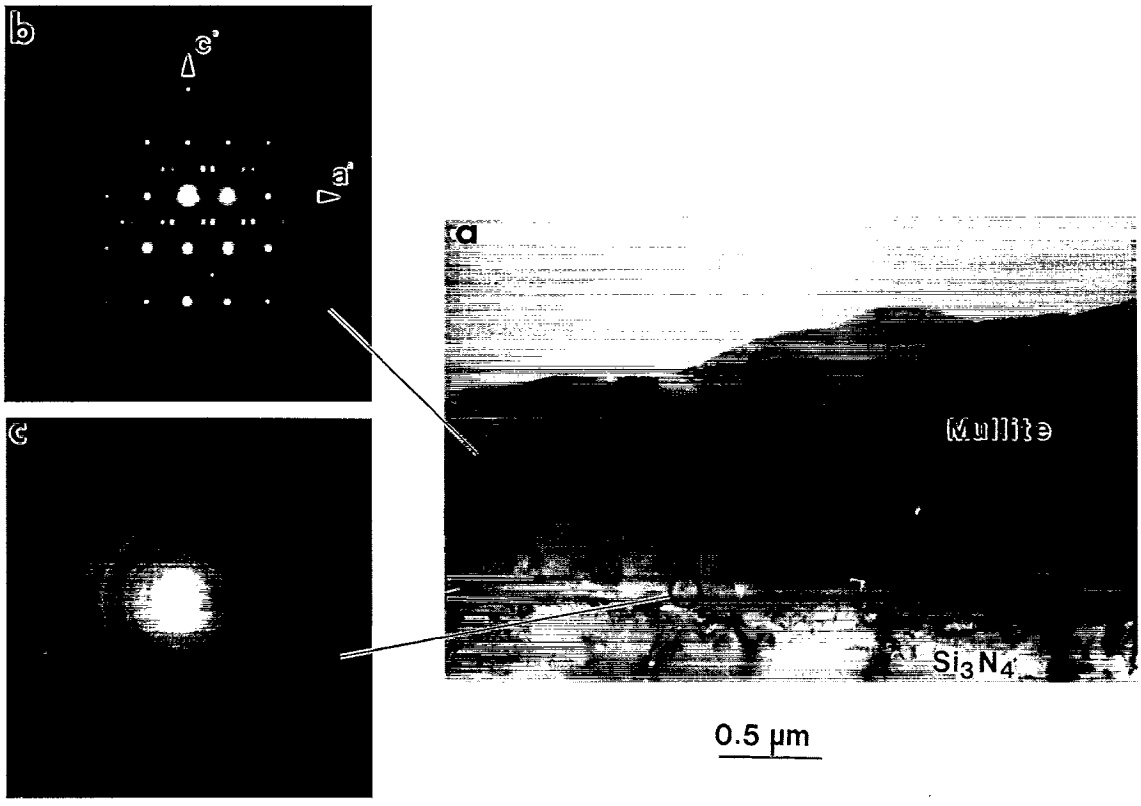


Fig. 3. (a) TEM micrograph of a mullite coating showing two distinct layers. Diffraction patterns from the (b) crystalline layer on top and (c) the nanocrystalline layer at the interface are included in the figure.

tion, marked as $T_2$ in Fig. 4 and bond with an oxygen atom at another $O_c$ site [16].

By the above described mechanism, increase in the Al/Si ratio in mullite leads to a corresponding increase in the number for oxygen vacancies in a unit cell, $x$. The maximum Al/Si ratio of 8, as observed in our STEM analysis, corresponds to $x = 0.67$ (Eq. (2)). This is the highest Al/Si ratio reported so far. This is in agreement with Burnham's theory that mullite solid solution could extend fully between sillimanite and pure alumina. It may be recalled that such graded coatings, with high Al/Si ratio at the surface are ideal for hot corrosion resistance.

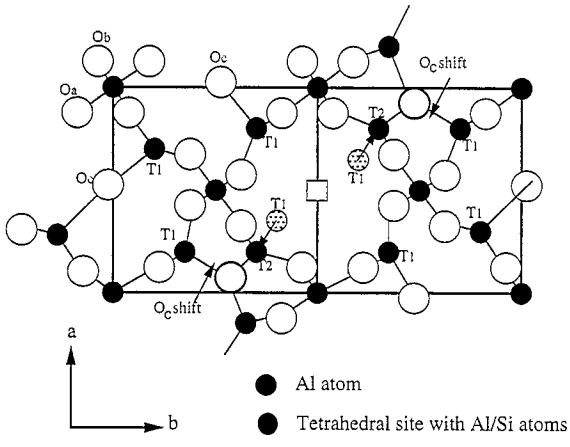


Fig. 4. Structural changes caused by oxygen vacancies in the mullite unitcell.

At high Al/Si concentrations, the oxygen vacancies order to minimize the free energy of the system. The ordering phenomenon has been investigated based on the extra reflections produced in electron diffraction patterns [5,13,14,16]. These reflections generally occur around the {h01} reflections, either in the form of satellites or as diffused streaks, depending on the extent of ordering. Greater ordering is recognized by sharper and more intense reflections. Fig. 5 shows {h01} diffraction spots at three different locations within the columnar layer of the coating. Close to the interface, the superlattice reflections are in the form of diffused streaks. This is consistent with D-mullite as reported by Agrell and Smith [13], in which there is poor ordering of oxygen vacancies. Towards the top of the coating, the satellite spots became sharper, indicating an ordering of oxygen vacancies. This is consistent with the presence of S-mullite [13].

Fig. 5 also shows that as the distance from the interface increased, the spacings between the satellite

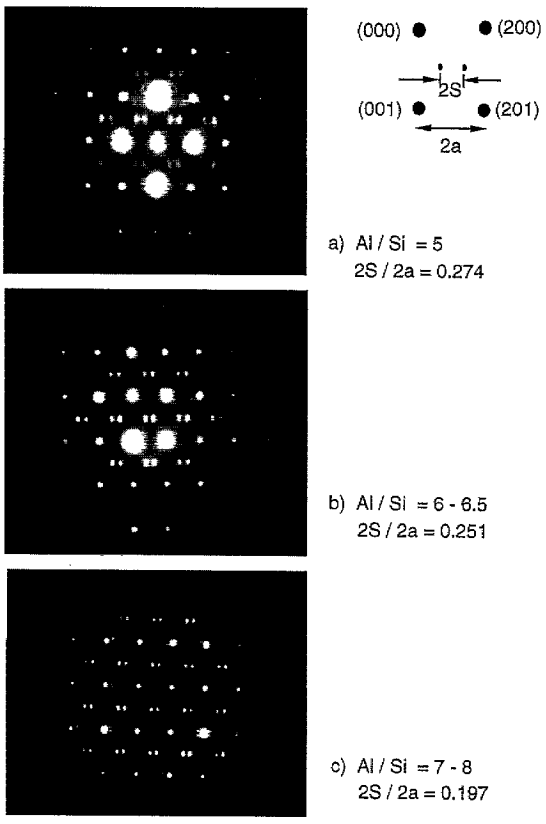


Fig. 5. Super lattice reflections in the {h01} reciprocal plane, at three different locations of the columnar layer of the coating.

spots decreased. In addition to the short range ordering in the unit cell, long range 2-D composition modulations have been reported in mullite [5]. These modulations are similar to those observed in spinodal decomposition reactions and reflect the equilibrium immiscibility of the alumina and silica phases at compositions different from stoichiometric mullite. The modulations give rise to domains that are separated by anti-phase domain boundaries (APB), oriented parallel to (100) planes [25,26]. The domain size (statistical average distance between APBs), is related to the spacing between the superlattice spots ($2S$ in Fig. 5) and is given as $1/2S$ [5]. In our study, this corresponds at a range of 1.5–2 nm. The maximum value reported before was 1.4 nm [5]. Cameron compared the superlattice structures of mullites with various Al/Si ratios. He plotted $S$ (taken as a fraction of lattic parameter $a$) as a function of $x$, the number of oxygen vacancies per unit cell (Fig. 6) [5]. The decrease in $S$, with increasing oxygen vacancy concentration is due to an increase in the inter-APB distance (larger domains).

Cameron found a linear relation between $S$ and $x$ (Fig. 6), for $x < 4.7$, after which, $S$ was essentially independent of $x$. However, our data fits fairly well with the extension of the linear region to higher values of $x$, implying a direct dependence of the domain width on oxygen vacancy concentration throughout the solid solubility range. Since, the formation of domains require long range ordering of vacancies, the process is diffusion controlled. The discrepancy between our observation and those reported by Cameron, is due to the much higher surface mobility in the CVD coatings compared to the bulk diffusion in Cameron's case.

Fig. 5(c) shows extra superlattice spots around {h01} reflections. These were seen only in regions of high Al/Si ratio. It is believed that this splitting of the spots is caused either by the formation of 3-D domains or due to the presence of twins [18]. In this study, some of the high Al concentration regions of the coating were found to be twinned. Additionally, the absence of extra superlattice reflections in the [100] diffraction patterns is an indication that the domain structure is only two-dimensional.

The compositional variation in mullite is also accompanied by a change in lattice parameters. Increasing the Al/Si ratio is accompanied by an increase of $a$ and a slight decrease of $b$ (Fig. 7). Therefore, the structure moves toward a tetragonal unit cell with increasing Al/Si ratio. This observation is in agreement with the earlier findings by other researchers [5,27]. These changes in the lattice parameters can be explained by vacancy ordering. Fig. 8 shows that the oxygen vacancies can either be randomly oriented or can be preferentially placed on the $b$-axis. the latter arrangement will cause a reduction in the lattice parameter $b$. However, this ordering will force the occupancy of only those tetrahedral sites ($T_1$ and $T_2$) which are closer to the $a$-axis. Since this forces occupied tetrahedra to be aligned next to each other along the $a$-axis, a small increase in the $a$-axis lattic parameter is energetically favorable.

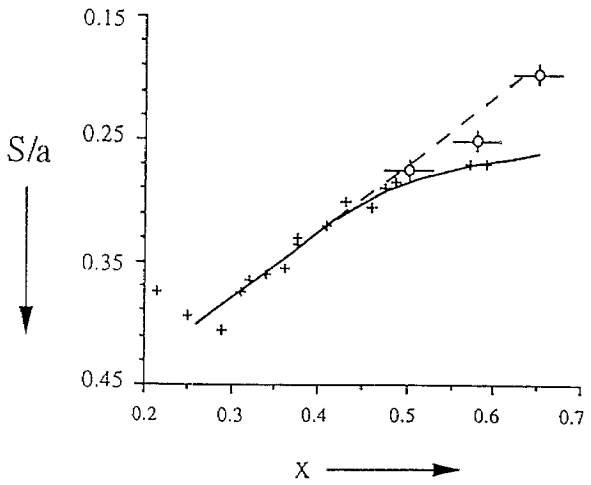


Fig. 6. Variation of the parameter $S$ with oxygen vacancy concentration ($x$). Results of this study are plotted as 'o' with accompanying error bars. The solid curve is plotted from Cameron's data, marked by '+'. Our data fits well with the linear extrapolation of Cameron's data at low values of $x$.

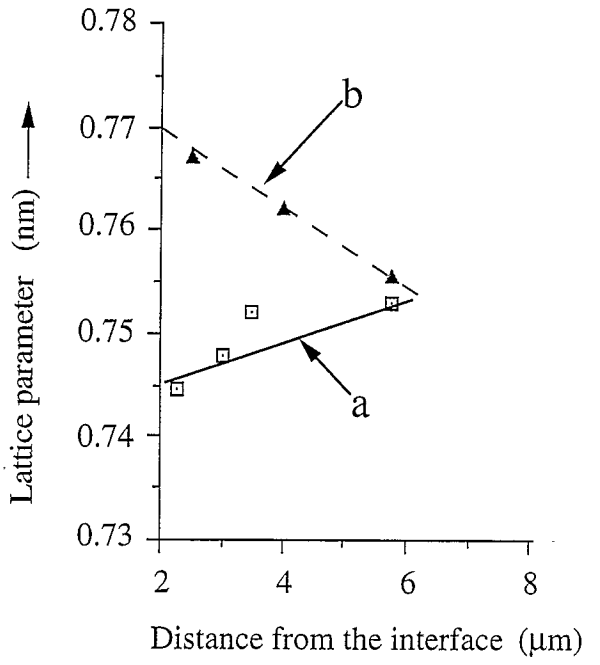


Fig. 7. The measured variation in the lattic parameter of mullite with distance from interface.

## 4. Conclusions

Adherent mullite coatings were deposited on SiC and $Si_3N_4$ substrates by a CVD process. The coatings were compositionally graded with the Al/Si ratio increasing from 2 at the interface to a value of 8 at the top of the coating. To our knowledge, this is the first report of such a graded mullite, within the same coating. Our observations support the earlier reports that a critical Al/Si ratio is required to nucleate mullite.

Evolution of non-stoichiometric mullite structure from sillimanite, by atomic substitution and formation of oxygen vacancies, is discussed. Our data indicate that by extension of the same mechanism, a pure alumina structure can be derived, as Burnham had proposed. The metastable mullite in our coatings, with the high oxygen vacancy concentration, was stabilized by the ordering of the oxygen vacancies and by the formation of domains. Ordering of oxygen vacancies in the mullite unit cell was deduced based on electron diffraction studies and this ordering was correlated with the observed changes in lattice parameters and Al/Si ratio. Formation of 2-D domains by long range ordering of oxygen vacancies was inferred from the images of APBs seen in electron diffraction patterns. The domain width was found to vary linearly with oxygen-vacancy concentration.

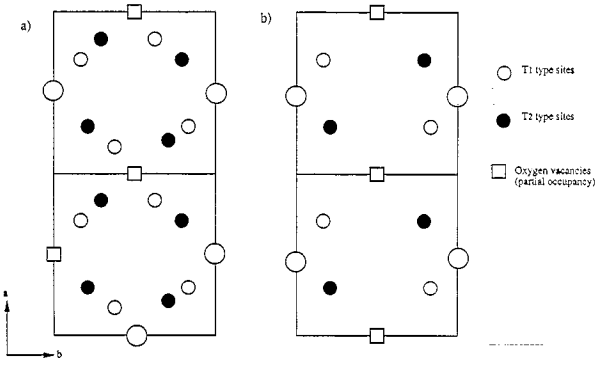


Fig. 8. Schematic of oxygen vacancies (a) distributed randomly and (b) ordered parallel to the *a*-axis in mullite with high Al/Si ratios.

## Acknowledgements

The authors would like to thank Professor V.K. Sarin and Dr R. Mulpuri for the very helpful discussion and for providing the CVD mullite coatings. The microscopy studies were carried out at the Electron Microscopy Facility in the Center for Materials Science and Engineering at MIT. This research was sponsored in part by the US Department of Energy under contract number DE-ACO5-840R21400.

## References

[1] CRC Materials Science and Engineering Handbook, in: J. Shackelford and W. Alexander (Eds.), CRC Press, Ann Arbor, MI, 1994.
[2] J.I. Federer, Adv. Ceram. Mater. 3 (1) (1988) 56.
[3] J.A. Pask, Mullite and Mullite Matrix Composites, in: S. Somiya, R.F. Davis and J.A. Pask (Eds.), Ceramic Transactions, Am. Ceram. Soc. 6 (1990) 1–12.
[4] S. Aramaki, R. Roy, J. Am. Ceram. Soc. 45 (5) (1962) 229–242.
[5] W.E. Cameron, Am. Mineralogist 62 (1977) 747–755.
[6] I.A. Aksay, J.A. Pask, Mullite and Mullite Matrix Composites, P, American Ceramic Society International Conference on Mullite, Tokyo, 1990, pp. 507–512.
[7] S. Prochazka, F.J. Klug, J. Am. Ceram. Soc. 66 (12) (1983) 874–880.
[8] D.X. Li, W.J. Thomson, J. Am. Ceram. Soc. 74 (10) (1991) 2382–2387.
[9] C.W. Burnham, Carnegie Institute Washington Year Book 63 (1964) 227–229.
[10] Powder Diffraction Files, International Centre for Diffraction Data, Swathmore, PA.
[11] T. Epicier, J. Am. Ceram. Soc. 74 (10) (1991) 2359–23566.
[12] S.H. Rahman, H.T. Weichert, Acta Cryst. B 46 (1990) 139–149.
[13] S.O. Agrell, J.V. Smith, J. Am. Ceram. Soc. 43 (2) (1960) 69–76.
[14] I.A. Aksay, D.M. Dabbs, M. Sarikaya, J. Am. Ceram. Soc. 74 (10) (1991) 2343–2358.
[15] D. Schryvers, K. Srikrishna, M.A. O'Keefe, G. Thomas, J. Mater. Res. 3 (6) (1988) 1355–1361.
[16] T. Epicier, M.A. O'Keefe, G. Thomas, Acta Cryst. A 46 (1990) 948–962.
[17] N. Morimoto, Y. Nakajima and M. Kitamuro, in: S. Somiya, R.F. Davis, J.A. Pask (Eds.), Ceramic Transactions, vol. 6, Am. Ceram. Soc., Westerville, OH, pp. 115–124.
[18] Y. Nakajima, P.H. Ribbe, Am. Mineralogist 66 (1981) 142–147.

[19] K.N. Lee, R.A. Miller, N.S. Jacobson, J. Am. Ceram. Soc. 78 (3) (1995) 705–710.
[20] T.M. Besmann, ORNL/TM 5775, Oak Ridge National Laboratory, Oak Ridge, TN, 1989.
[21] Rao P. Mulpuri, Vinod K Sarin, J. Mater. Res. 11 (6) (1996) 1315–1324.
[22] Rao P. Mulpuri, Chemical Vapor Deposition of Mullite Coatings On Silicon Based Ceramics for High Temperature Applications, Doctoral thesis, Department of Manufacturing Engineering, Boston University, 1995.
[23] S. Sundaresan, I.A. Aksay, J. Am. Ceram. Soc. 73 (10) (1991) 2388–2392.
[24] B.B. Ghate, D.P.H. Hasselman, R.M. Spriggs, Ceramic Bulletin 52 (9) (1993) 670–672.
[25] D.G.W. Smith, J.D.C. McConnell, Mineral. Mag. 35 (1966) 810–814.
[26] Y. Nakajima, N. Morimoto, E. Watanabe, Proc. Jpn. Acad. 51 (1975) 173–178.
[27] J. Ossaka, Nature (London) 19 (4792) (1961) 1000–1001.